

probe accurately reflects the value of the average  $\tau_D$  for anisotropic motion, plots of  $\log \tau_c$  vs.  $(T - T_g)$ , as shown in Figure 16, were constructed. These diagrams show that the bulkier probe D can be considered to reflect the glass transition at  $T_{50G}$ . However, it is obvious from Figures 10 and 16 that this  $T_{50G}$  value is correlated with the  $T_{gl}$ -relaxation process and not with the  $T_{gu}$  relaxation, as concluded by Kumler and Boyer.<sup>27</sup> When the theory of Kusumoto et al.<sup>28</sup> is used, a value of  $f \approx 1$ , eq 11, is found, indicating that the volume of the polymer segments undergoing  $\beta_L$  relaxation is approximately that of probe D. At about 418 and 408 K for probes C and D, respectively, the experimental ratio  $(R_+ + R_- - 2)/(R_+ - R_-)$  approaches the theoretical values calculated for radicals undergoing isotropic reorientation.<sup>6</sup> Figures 10 and 16 show that both probes C and D respond to the  $T_{gu}$ -relaxation process.

**Registry No.** PVDF (homopolymer), 24937-79-9; (VDF)·(TFE) (copolymer), 25684-76-8; (VDF)·(CTFE) (copolymer), 9010-75-7.

## References and Notes

- Boyer, R. F. *J. Polym. Sci., Polym. Symp.* **1975**, *50*, 189.
- McBrierty, V. J.; Douglass, D. C.; Weber, T. A. *J. Polym. Sci., Polym. Phys. Ed.* **1976**, *14*, 1271.
- Enns, J. B.; Simha, R. *J. Macromol. Sci., Phys.* **1977**, *B13*, 11.
- Léonard, C.; Halary, J. L.; Monnerie, L.; Micheron, F. *Polym. Bull. (Berlin)* **1984**, *11*, 195.
- Tormala, P. *J. Macromol. Sci., Rev. Macromol. Chem.* **1979**, *C17*, 297.
- Cameron, G. G.; Bullock, A. T. In "Developments in Polymer Characterisation"; Dawkins, J. V., Ed.; Applied Science: London, 1982; p 107.
- Anufrieva, E. V.; Gotlib, Yu Ya *Adv. Polym. Sci.* **1981**, *40*, 1.
- Monnerie, L. In "Static and Dynamic Properties of the Polymeric Solid State"; Pethrick, R. A.; Richards, R. W., Eds.; Reidel: London, 1982; p 383.
- Jarry, J. P.; Monnerie, L. *Macromolecules* **1979**, *12*, 925.
- Pinaud, F.; Jarry, J. P.; Sergot, P.; Monnerie, L. *Polymer* **1982**, *23*, 1575.
- Valeur, B.; Monnerie, L. *J. Polymer Sci., Polym. Phys. Ed.* **1976**, *14*, 11.
- "Spin Labeling—Theory and Applications"; Berliner, L. J., Ed.; Academic Press: New York, 1976.
- Freed, J. H.; Bruno, G. V.; Polnaszek, C. F. *J. Phys. Chem.* **1971**, *75*, 3385.
- Freed, J. H. In "Spin Labeling—Theory and Applications"; Berliner, L. J., Ed.; Academic Press: New York, 1976; p 53.
- Hwang, J. S.; Mason, R. P.; Hwang, L. P.; Freed, J. H. *J. Phys. Chem.* **1975**, *79*, 489.
- Gade, S.; Chow, A.; Knispel, R. *J. Magn. Reson.* **1980**, *40*, 273.
- Smith, P. M. *Eur. Polym. J.* **1979**, *15*, 147.
- Kovarskii, A. L.; Vasserman, A. M.; Buchachenko, A. L. *Vysokomol. Soedin., Ser. A* **1971**, *13*, 1647.
- Meurisse, P.; Friedrich, C.; Dvolaitzky, M.; Lauprêtre, F.; Noël, C.; Monnerie, L. *Macromolecules* **1984**, *17*, 72.
- Goldman, S. A.; Bruno, G. V.; Freed, J. H. *J. Phys. Chem.* **1972**, *76*, 1858.
- Kuznetsov, A. N.; Ebert, B. *Chem. Phys. Lett.* **1974**, *25*, 342.
- Wasserman, A. M.; Alexandrova, T. A.; Buchachenko, A. L. *Eur. Polym. J.* **1976**, *12*, 691.
- Monnerie, L.; Jarry, J. P. *Ann. N. Y. Acad. Sci.* **1981**, *366*, 328.
- Quesel, J. P. Docteur-Ingénieur Thesis, Paris, 1982.
- Ferry, J. D. In "Viscoelastic Properties of Polymers"; Wiley: New York, 1970.
- Although Voltalefs 3700 and 5500 are amorphous polymers, the  $T_g$  relaxation is called " $\beta$  process" to make easier the comparison with PVDF, a semicrystalline polymer, which exhibits premelting process [ $T_{ac}$  or  $\alpha$ ], upper glass transition [ $T_{gu}$ ], lower glass transition [ $T_{gl}$ ] ( $\beta$  processes), and local mode chain motion [ $T < T_g$  or  $\gamma$  process].
- Kumler, P. L.; Boyer, R. F. *Macromolecules* **1976**, *9*, 903.
- Kusumoto, N.; Sano, S.; Zaitzu, N.; Motozato, Y. *Polymer* **1976**, *17*, 448.
- Bueche, F. In "Physical Properties of Polymers"; Wiley: New York, 1962.
- Pajot-Augy, E.; Bokobza, L.; Monnerie, L.; Castellan, A.; Bouas-Laurent, H. *Macromolecules* **1984**, *17*, 1490.
- Pham-Van-Cang, C.; Bokobza, L.; Monnerie, L.; Vandendriessche, J.; De Schryver, F. C. Submitted to *Polymer*.
- Osaki, S.; Ishida, Y. *J. Polym. Sci., Polym. Phys. Ed.* **1974**, *12*, 1727.
- Yano, S. *J. Polym. Sci., Polym. Phys. Ed.* **1970**, *8*, 1057.
- Hedvig, P. "Dielectric Spectroscopy of Polymers"; Adam Hilger: Budapest, 1977.
- Kakutani, H. *J. Polym. Sci., Polym. Phys. Ed.* **1970**, *8*, 1177.
- Boyer, R. F.; Kumler, P. L. In "Structure and Motion in Polymer Glasses", 10th Europhysics Conference on Macromolecular Physics; Thomas, G.; Merz, W. J., Eds.; European Physical Society: Petit-Lancy, Switzerland, 1980; p 190.
- Bullock, A. T.; Cameron, G. G.; Smith, P. M. (a) *J. Polym. Sci., Polym. Phys. Ed.* **1973**, *11*, 1263. (b) *Eur. Polym. J.* **1975**, *11*, 617.
- Kumler, P. L.; Keinath, S. E.; Boyer, R. F. *Polym. Prepr. (Am. Chem. Soc., Div. Polym. Chem.)* **1976**, *17*, 28.

## Two-Dimensional Nuclear Magnetic Resonance Analysis of Poly(vinyl chloride) Microstructure

Peter A. Mirau\* and Frank A. Bovey

AT&T Bell Laboratories, Murray Hill, New Jersey 07974. Received June 18, 1985

**ABSTRACT:** One- and two-dimensional heteronuclear  $^1\text{H}$ - $^{13}\text{C}$  and homonuclear  $^1\text{H}$  NMR experiments have been examined for their usefulness in establishing stereochemical sequence assignments in poly(vinyl chloride). Correlation via the  $^1\text{H}$ - $^{13}\text{C}$  coupling leads to increased resolution in both the proton and carbon spectra, and stereochemical assignments may be made by inspection of the 2D map. Homonuclear correlation via three-bond scalar coupling (COSY) may be used to make some of the stereochemical assignments based on the proton data alone. Differences in the magnitudes of the coupling constants may be exploited to uniquely define some of the stereochemical spin systems by utilizing the correlations via double-quantum coherences. Longer range correlations (relayed coherence transfer) define larger segments of the polymer backbone. These studies show that many of the techniques developed for small molecules are applicable to polymer systems and the complete stereochemical resonance assignments may be obtained by the utilization of a number of 2D experiments.

## Introduction

The physical properties of synthetic polymers depend on their microstructure and conformational properties, and methods for elucidation of the structure are an important part of polymer research. NMR is a powerful tool for polymer characterization since the NMR parameters

(chemical shift, coupling constants, and relaxation rates) depend on the local environment and dynamics of the nuclei.<sup>1,2</sup> High resolution  $^1\text{H}$  NMR is a particularly attractive tool due to its high observing sensitivity, but it is somewhat limited due to relatively broad lines and peak overlap. One way to overcome these limitations is to use

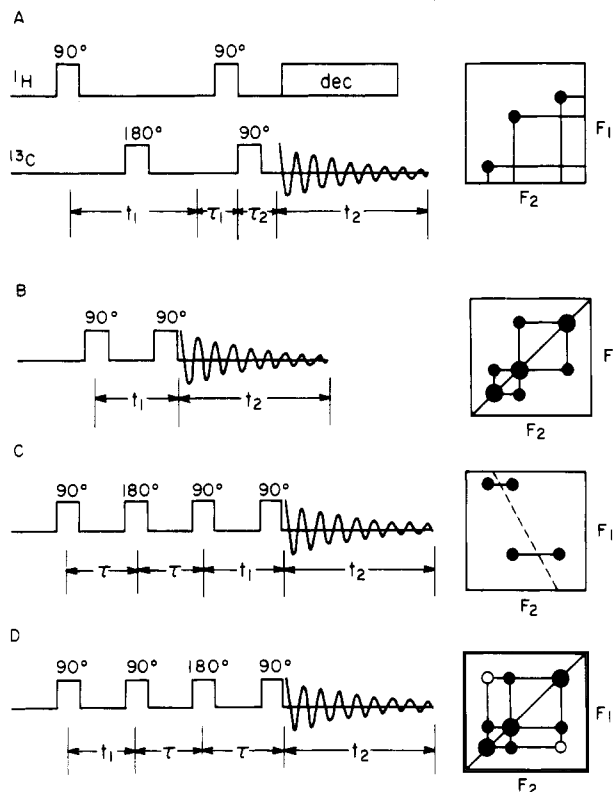


**Figure 1.** Pulse sequences and correlation diagrams for (A) heteronuclear chemical shift correlation, (B) COSY, (C)  $^1\text{H}$ - $^1\text{H}$  double-quantum correlation, and (D) relayed coherence transfer (RCT). The time variable  $t_1$  is systematically incremented throughout the experiment. The normal spectrum appears along the  $F_2$  axis, while the meaning of the  $F_1$  axis depends on the pulse sequence. See text for more detail.

two-dimensional (2D) NMR.<sup>3,4</sup> This approach has been successfully used in the study of biopolymers<sup>5</sup> and has recently been applied to high molecular weight synthetic polymers.<sup>6-13</sup> There are many 2D experiments which differ in the type of interaction used to correlate different regions of the spectrum. Most experiments utilize correlations by either through-bond scalar interactions or through-space dipolar interactions.<sup>3</sup>

In this study we have examined a number of 2D techniques to determine their usefulness in making stereochemical sequence assignments in synthetic polymers. We chose to observe poly(vinyl chloride) because it has been extensively studied and the  $^1\text{H}$  and  $^{13}\text{C}$  chemical shifts are known to be sensitive to stereochemical configuration.<sup>1,2,14,15</sup> Assignment of the proton resonances in poly(vinyl chloride) is difficult since the methylene protons in the various stereosequences are not resolved and methine-methylene coupling patterns may be quite complex.<sup>2,14</sup> We report here that it is possible to solve such assignment problems by utilizing the 2D experiments designed for structure elucidation in small molecules. The success of this approach is due, in part, to the fact that the polymer backbone is sufficiently mobile to give rise to line widths that are less than the coupling constants. While no single 2D experiment provides all of the desired information, the combination of several techniques may lead to the complete assignments of stereochemical or copolymer sequences.

The pulse sequences and correlation maps for several hetero- and homonuclear 2D experiments are shown in Figure 1.<sup>4</sup> All 2D experiments consist of a series of pulses and intervals and contain the intervals  $t_1$  and  $t_2$ . The value of  $t_1$  is systematically incremented throughout the course

of the experiment, and  $t_2$  is the period in which the free induction decay is acquired. Double Fourier transformation with respect to  $t_1$  and  $t_2$  yields the 2D data matrix with the frequency variables  $F_1$  and  $F_2$ . The normal spectrum appears in the  $F_2$  dimension, and the information appearing in the  $F_1$  dimension depends on the pulse sequence.

**Heteronuclear Chemical Shift Correlation.** The pulse sequence used to generate the 2D map that correlates the carbon and proton chemical shifts (Figure 1A) consists of a series of pulses applied at the carbon and proton frequencies.<sup>4,16,17</sup> The carbon signal is recorded during  $t_2$  with broad-band proton decoupling. Following double Fourier transformation, a 2D data matrix is obtained with the carbon chemical shifts along one axis ( $F_2$ ) and the proton chemical shifts along the other ( $F_1$ ). Connectivities are established by noting the frequencies at which the peaks appear along both the carbon and proton axes. Correlations via the C-H bond are most efficient when the delay period  $\tau_1$  is equal to  $1/2J_{\text{CH}}$ , where  $J_{\text{CH}}$  is the one-bond C-H coupling constant. The value of  $\tau_2$  is set to  $1/3J_{\text{CH}}$  when proton-decoupled spectra are recorded.<sup>4</sup>

**Homonuclear Correlations.** The pulse sequence and correlation diagram for correlation via homonuclear scalar coupling (COSY)<sup>4,18</sup> are shown in Figure 1B. The frequency axes  $F_1$  and  $F_2$  contain the  $^1\text{H}$  chemical shifts while the spectrum appears along the diagonal ( $F_1 = F_2$ ). Smaller off-diagonal peaks arise from scalar coupling and reveal the connectivity within stereosequences.

Much of the same information can be obtained from correlations via double-quantum coherences. The pulse sequence for the  $^1\text{H}$ - $^1\text{H}$  double-quantum correlation<sup>19</sup> experiment is shown in Figure 1C. In this case, the normal spectrum appears along the  $F_2$  axis and  $F_1$  is the double-quantum frequency axis (i.e.,  $F_1 = 2F_2$ ). The 2D spectrum also differs from the COSY spectrum in that (1) the peaks are correlated horizontally, (2) there are no resonances on the diagonal, and (3) the intensities depend on the coupling constants and the delay time  $\tau$ .

Figure 1D shows the pulse sequence and diagram for nuclear correlation via relayed coherence transfer.<sup>20-22,25</sup> The format is similar to that for COSY (Figure 1B) except that cross peaks are observed not only for directly coupled spin systems but also for indirectly coupled systems (i.e., next nearest neighbors). Like the  $^1\text{H}$ - $^1\text{H}$  double-quantum correlation, the efficiency of magnetization transfer depends on the proper choice of  $\tau$ .

## Materials and Methods

Poly(vinyl chloride) (MW 83 000) and deuterated solvents were obtained from Aldrich Chemical Co. and used without further purification. The samples typically contained 10% poly(vinyl chloride) in 90% 1,2,4-trichlorobenzene/10% chlorobenzene- $d_4$  for  $^{13}\text{C}$  measurements and 5-10% poly(vinyl chloride) in 80% benzene- $d_6$ /20% chlorobenzene- $d_5$  for  $^1\text{H}$  measurements.

NMR experiments were performed at 500 MHz for  $^1\text{H}$  and 125 MHz for  $^{13}\text{C}$  on a JEOL GX-500 spectrometer. The experiments typically required 9-12 h for data accumulation and 1 h for data processing and plotting. In most experiments 256 1K spectra were acquired and the data matrix was zero-filled to  $512 \times 1024$ . The matrix was apodized with a combination of trapezoidal and exponential multiplication (1-3 Hz), and absolute value spectra are presented. All but the relayed coherence transfer spectra were acquired with quadrature detection in both domains.

## Results

**$^1\text{H}$  and  $^{13}\text{C}$  NMR of Poly(vinyl chloride).** The  $^1\text{H}$  and  $^{13}\text{C}$  spectra of poly(vinyl chloride) (Figure 2) show two groups of resonances which arise from the methine and from the methylene groups. Within these groups of resonances there are peaks due to the stereochemical se-

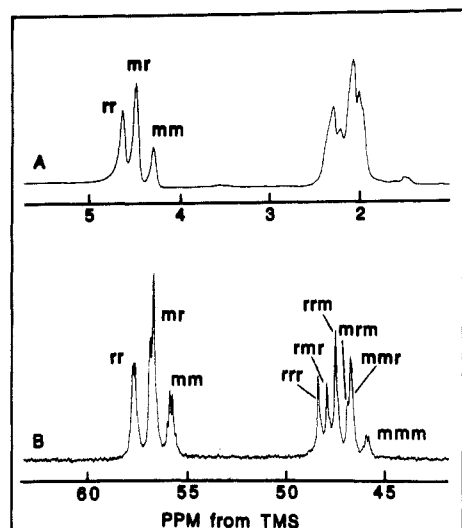


**Figure 2.** The 500-MHz  $^1\text{H}$  and 125-MHz  $^{13}\text{C}$  spectra of poly(vinyl chloride) at 65  $^\circ\text{C}$ .

quence effects, as has been previously discussed.<sup>1,2,14,15</sup> The  $^{13}\text{C}$  spectrum is better resolved than is the  $^1\text{H}$  spectrum and shows that all stereosequences are not present to the same extent. From these data alone it is not possible to determine the resonance assignments.

**Heteronuclear Chemical Shift Correlations.** Two-dimensional heteronuclear chemical shift correlation can be used to correlate the  $^{13}\text{C}$  resonance with the  $^1\text{H}$  resonance from the directly bonded proton using pulse sequence 1A. Most efficient correlation is obtained when the delay  $\tau_1$  is set to  $1/2J_{\text{CH}}$ . Since the  $J_{\text{CH}}$  is greater for the chlorinated methine (150 Hz) than the methylene (125 Hz), we chose to optimize the correlation for the average value of  $J_{\text{CH}} = 130$  Hz. Figure 3 shows the 2D correlation map for poly(vinyl chloride) at 90  $^\circ\text{C}$ . Before considering in detail the assignments in poly(vinyl chloride), we note some features of the correlation that may be common to the study of all polymers by carbon-proton chemical shift correlation.

i. The resolution in the 2D spectrum is better than in either the  $^{13}\text{C}$  or  $^1\text{H}$  spectrum alone. Resonances that overlap in both the  $^1\text{H}$  and  $^{13}\text{C}$  spectrum may be resolved in the 2D correlation map. This effect is most obvious in the inset of Figure 3, which shows the  $^{13}\text{C}$ - $^1\text{H}$  correlation for the methylene region. The peaks are unresolved in the proton spectrum (Figure 2) but in the  $^1\text{H}$ - $^{13}\text{C}$  correlation spectrum separate resonances are observed for each stereosequence.

ii. There is no one-to-one correlation between the  $^{13}\text{C}$  and  $^1\text{H}$  chemical shifts; that is, the highest field  $^{13}\text{C}$  resonance is not necessarily correlated with the highest field  $^1\text{H}$  peak. This result shows that the same factors do not influence the  $^{13}\text{C}$  and  $^1\text{H}$  chemical shifts to the same extent. The  $^1\text{H}$  chemical shifts are determined by the carbon type (methyl, methine, methylene) and the inductive effects due to substituents and ionizable groups.  $^{13}\text{C}$  chemical shifts are also sensitive to these factors but also to the rotational isomeric state of the polymer.<sup>23,24</sup> The so-called  $\gamma$ -effect is well documented in poly(vinyl chloride) and other polymer systems.<sup>24</sup>

iii. The 2D correlation map has the potential to reveal some stereochemical consequences that are invisible in the  $^{13}\text{C}$  spectrum and obscured in the  $^1\text{H}$  spectrum. For example, the methylene protons in the rmr tetrad are non-equivalent but unresolved due to overlap with the other stereosequences. Such peaks are distinguished in the 2D correlation map by the fact that the  $^{13}\text{C}$  resonance is

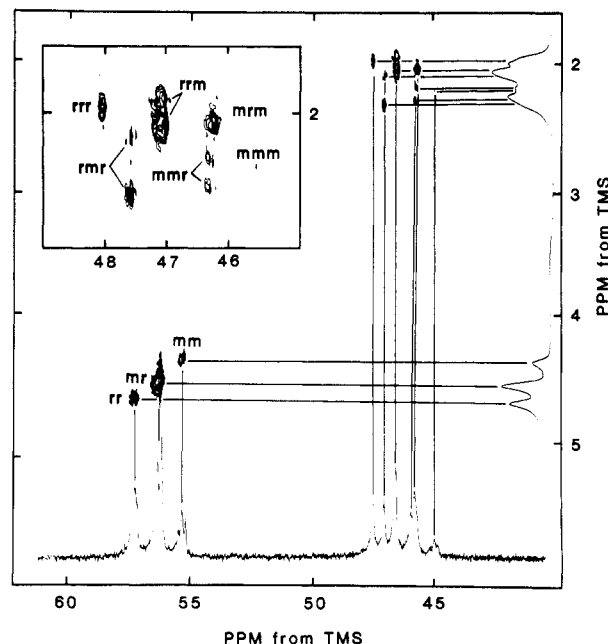


**Figure 3.** Heteronuclear  $^1\text{H}$ - $^{13}\text{C}$  correlation spectrum of poly(vinyl chloride) at 65  $^\circ\text{C}$  obtained with the pulse sequence 1A. The delays  $\tau_1$  and  $\tau_2$  were 3.8 and 2.5 ms, and the  $^{13}\text{C}$  and  $^1\text{H}$  sweep widths were 4 kHz. The inset plot shows an expansion of the methylene region. 256 spectra were acquired in 1K points, and the matrix was zero-filled to  $512 \times 1\text{K}$ . Trapezoidal multiplication and line broadening were applied in both dimensions prior to Fourier transformation.

correlated with two peaks in the  $^1\text{H}$  spectrum.

The  $^1\text{H}$ - $^{13}\text{C}$  correlated 2D spectrum of poly(vinyl chloride) shows all of these features: the 2D spectrum is better resolved, there is no one-to-one correlation between the chemical shifts of the  $^1\text{H}$  and  $^{13}\text{C}$ , and some of the  $^{13}\text{C}$  peaks (rmr, rrm, and mmr) are correlated with more than one proton resonance. The resonance assignment strategy from the 2D experiments depends to a large degree on how much information is known about the polymer. If, as in the case of poly(vinyl chloride), the  $^{13}\text{C}$  resonances have been assigned,<sup>1,15</sup> then assignment of the proton resonances proceeds following inspection of the 2D map. If this information is not available, both the hetero- and homonuclear correlation information is required.

With the utilization of the known  $^{13}\text{C}$  chemical shifts of poly(vinyl chloride), Figure 3 summarizes the  $^1\text{H}$  chemical shift assignments. In the methine region the rr, mr, and mm triads show the same relative ordering along both the  $^{13}\text{C}$  and  $^1\text{H}$  axes. Note that the  $^{13}\text{C}$  spectrum has fine structure within each peak, but the resolved resonances are correlated with protons that have the same chemical shift, so separate peaks are not observed in the proton spectrum. In the methylene region there is no simple relationship to the ordering of the  $^1\text{H}$  and  $^{13}\text{C}$  chemical shifts. The chemical shifts of the protons assigned via the 2D correlation agree with those previously determined by more conventional methods.<sup>14</sup>

**Homonuclear Correlations.** In many polymer spectra, the  $^{13}\text{C}$  chemical shifts are not known, so assignments must be made via proton-proton interactions. In vinyl polymers there is an array of contiguous coupled spins along the polymer chain and we may take advantage of the methine-methylene three-bond coupling to correlate both the nearest and next nearest neighbors. We find that several types of 2D experiments utilizing this interaction are necessary to establish the proton assignments.

Figure 4 shows the 2D  $^1\text{H}$  COSY spectrum of poly(vinyl chloride) at 65  $^\circ\text{C}$ . The connectivities between the methine

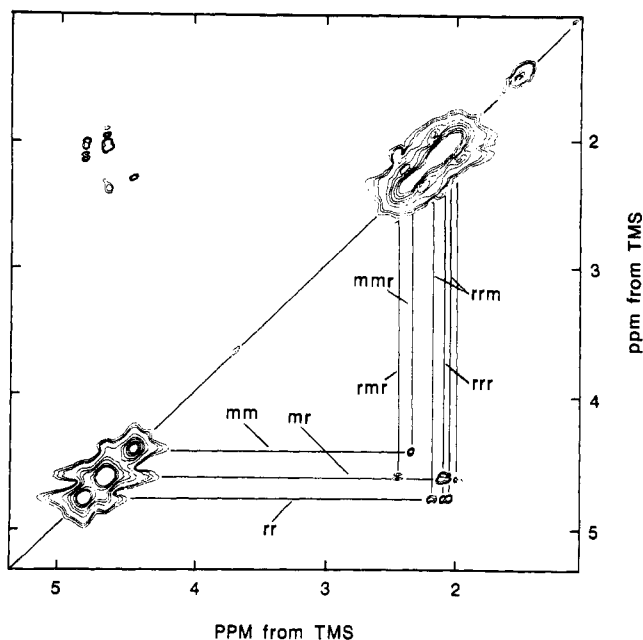


**Figure 4.** The 500-MHz COSY spectrum of poly(vinyl chloride) at 65 °C obtained with pulse sequence 1B, except that the two radio-frequency pulses were compensated for pulse inhomogeneities. See Figure 3 for details.

and methylene groups within a given stereo sequence are revealed by the cross peaks in the lower left (and upper right) quadrants of the COSY spectrum. The intensities of the cross peaks depend on a number of features, including the coupling constants, the complexity of the coupling pattern, the relaxation rates, and the relative abundance of a given stereosequence. In an absorption phase display (rather than the absolute value mode display shown here) the antiphase nature of the lines in the cross peak multiplet are clearly visible.<sup>4,7</sup> This leads to a cancellation of the cross peaks when the line widths approach the magnitude of the coupling constant. For polymers, where the line widths are typically on the order of 2–5 Hz, small coupling constants and complex multiplets will diminish the cross peak intensity.

The solid lines in Figure 4 show the correlation between triad and the tetrad resonances. Two correlations are expected for rr (rrr and mrr) and mm (mmm and mmmr), while four are expected for mr (mrr, mrm, rmr, and mmmr).<sup>9</sup> In those cases where the methylene protons are non-equivalent, additional correlations are expected. Inspection of Figure 4 shows that there are fewer cross peaks than expected. However, the spectrum can be partially assigned from consideration of the number of cross peaks. The <sup>13</sup>C NMR spectra (Figure 2) show that the mmm sequences are less frequent than mmmr and therefore will give rise to only small cross peaks. The highest field triad resonance has a single cross peak into the methylene region and must be due to the mm–mmr interaction. At lower contour levels (not shown) the peak due to the mm–mmm interaction becomes visible. The largest number of cross peaks are to the middle triad sequence, so this resonance must be assigned to mr. The lowest field methine peak is due to rr and is expected to show cross peaks to mrr and rrr.

Because of the missing cross peaks and the extensive overlap, it is not possible to completely assign the proton spectrum of poly(vinyl chloride) from the COSY spectrum alone. Additional information about peak assignments may be obtained from measuring the <sup>1</sup>H–<sup>1</sup>H double-quantum spectrum of poly(vinyl chloride) with different delay times, as shown in Figure 5. This experiment

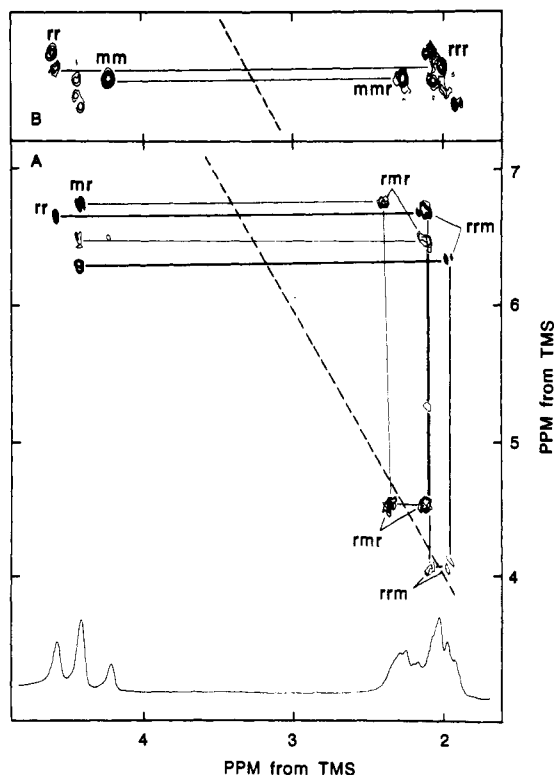


**Figure 5.** The 500-MHz <sup>1</sup>H–<sup>1</sup>H double-quantum spectra of poly(vinyl chloride) at 65 °C (pulse sequence 1C) obtained with several delay times of 8 and 18 ms. (A) shows the complete spectrum for  $\tau = 8$  ms. (B) shows an expansion of the methine–methylene correlations for  $\tau = 18$  ms. The dotted line shows the axis at  $F_2 = 2F_1$ .

correlates the coupled resonances via the single- and double-quantum coherences and has several practical advantages over the COSY spectrum in terms of resolution, ease of interpretation, and the ability to emphasize certain couplings. The increase in resolution is due to the correlation of single- and double-quantum coherences, so the peaks appear at their usual frequency in  $F_2$  but at the sum of the frequencies of the coupled spins in  $F_1$ . This may lead to a two-fold increase in resolution in the  $F_1$  domain. The spectra are easier to interpret because the coupled resonances are related horizontally and appear equidistant from the frequency axis at  $F_1 = 2F_2$ , as shown by the dotted line in Figure 5. The <sup>1</sup>H–<sup>1</sup>H double-quantum spectrum also lacks the intense diagonal peaks of the COSY spectrum, and correlation of peaks close in frequency is possible. The intensities of the correlated peaks depend on the delay time  $\tau$  (sequence 1C) through the transfer function  $f = \sin(2\pi J\tau) e^{-2\tau/T_2}$  for a two spin system. More complex coupling patterns lead to a more complex time dependence and diminished correlations. We may exploit this dependence of the peak intensities on the coupling constants to obtain information about stereosequences which have different couplings.

Figure 5, parts A and B, show the <sup>1</sup>H–<sup>1</sup>H double-quantum spectrum of poly(vinyl chloride) at 65 °C for two different delay times, 8 and 18 ms. At 8 ms the spectrum emphasizes those peaks with larger coupling constants and simpler coupling patterns. The strongest coupling in poly(vinyl chloride) is between the geminally coupled nonequivalent methylene protons (15 Hz).<sup>2</sup> The methine–methylene coupling depends on stereosequence, and the  $J_{\alpha\beta}$  coupling constants for the r-centered sequences are 11 and 2 Hz and are 6.5 and 7.5 Hz for the m-centered ones.<sup>14</sup> Shorter  $\tau$  values would emphasize correlations within the methylene groups and the r-centered ster-

sequences. Figure 5A shows that there are two groups of peaks that appear in the  $^1\text{H}$ - $^1\text{H}$  double-quantum spectrum. The  $F_1$  domain around 4 ppm shows the correlations between the methylene resonances that are close in frequency; these must be due to the geminally coupled methylene protons. Peaks due to methine-methylene coupling appear in their normal frequencies along  $F_2$  and around 6 ppm in the  $F_1$  domain. To illustrate how the double-quantum spectroscopy may be used to assign polymer spectra, we have drawn bold lines connecting the correlations within the rrm spin system, and lighter lines within the rmr system. First, we will trace through the rrm spin system. The highest field correlation in  $F_1$  (bottom right corner) shows the connection between the geminally coupled methylene protons in the rrm tetrad. Other correlations to these protons appear at the same frequency in  $F_2$  and are connected as shown by the vertical lines. The vertical lines are connected to two peaks that show correlations between the methine and methylene region; one is correlated to the rr and one to the mr triad. Since only the rrm tetrad can show methylene correlations to the mr and rr triads, this correlation uniquely defines the rrm spin system. In a completely analogous way, the correlations may be traced through for the rmr spin system. In contrast to the rrm correlation, the rmr tetrad will show horizontal correlations only to mr triad peaks. Figure 5b shows the tetrad-triad region of the double-quantum spectrum obtained with an 18-ms delay time. The spectrum shows the peaks seen in the spectrum with an 8-ms delay and a number of additional peaks that are connected by horizontal lines. At 18 ms a strong and a weak correlation between the mm methine and methylene regions are found. These peaks must be the mm-mm and the mm-mm correlations. A new peak to the rr triad reveals the chemical shift of the rrr tetrad sequence. Thus, with a combination of the COSY and  $^1\text{H}$ - $^1\text{H}$  double-quantum spectra gathered at different delay times, some of the spin systems are unambiguously correlated; by a process of elimination the other peaks may be assigned.

The key to assignments by such correlation techniques relies on the ability of the experiments to uniquely define the interactions between spin systems. In addition to COSY and double-quantum correlation, there are other correlation schemes that may also reveal the connectivities. Figure 6 shows the relayed coherence transfer<sup>19,25</sup> (RCT) spectrum of poly(vinyl chloride) (sequence 1D), which was obtained with a 25-ms delay time. The RCT spectrum shows correlations not only between directly bonded units but also between next nearest neighbors. In addition to the methine-methylene correlations seen in the COSY spectrum, peaks due to methine-methine and methylene-methylene relayed coherences are also expected for poly(vinyl chloride). The relayed methine-methine correlations, connected by the solid lines in Figure 6, show the connectivities between the rr and mr and the mm and mr triads. This pattern defines the mr triads, since the mm and rr triads cannot be correlated to each other. The mm and mr triads are related through the mmr tetrad, which contains an mm and mr triad. Similarly, the mr and rr are related through the rrm tetrad. Also note that the mr-mm relayed cross peak is more intense than the mr-rr one. This reflects the dependence of the transfer efficiency on the  $J_{\alpha\beta}$  coupling constants. Relayed methylene-methylene correlations are expected but are too near the diagonal to give rise to clearly resolved peaks. This pulse sequence should be extremely useful as the starting point for the analysis of the spectra of more complex molecules, such as copolymers.

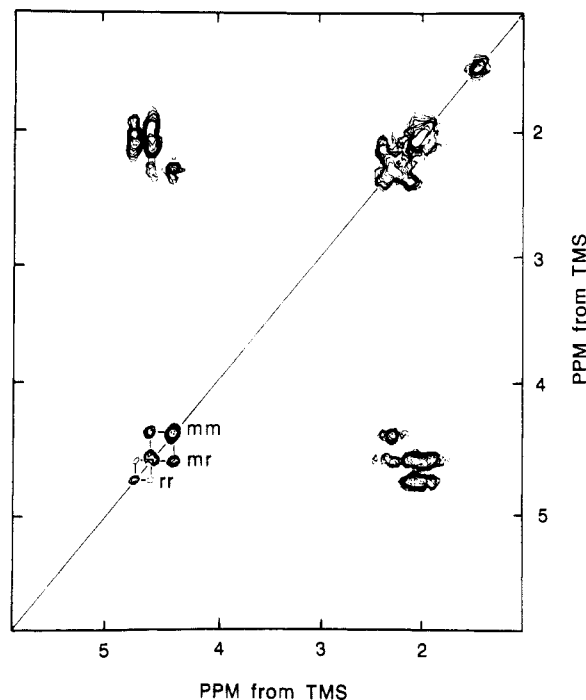


Figure 6. The  $^1\text{H}$  relayed coherence transfer (RCT) spectrum of poly(vinyl chloride) (pulse sequence 1D) with a delay time of 25 ms.

## Discussion

These studies show that a variety of two-dimensional NMR approaches have the potential to yield information about the resonance assignments and microstructure of polymers. This is due in part to the fact that the polymer chain is sufficiently mobile that the lines are relatively sharp (3–5 Hz), and the relaxation rates are slow compared to the coupling constants. Random coil polymers like poly(vinyl chloride) are thus amenable to analysis by the two-dimensional correlation techniques, which were originally developed for smaller molecules. This situation will not apply to structure-forming polymers (such as a helical polypeptide) longer than about 100 monomer units.<sup>5</sup>

We chose to test the applicability of 2D techniques on poly(vinyl chloride) because of the large body of existing work. Poly(vinyl chloride) is one of the more difficult cases on which to test the 2D approach because there is extensive peak overlap, and the methine-methylene coupling patterns are complex due to the nonequivalence of the methylene protons in some stereosequences. The results show that the 2D approach will be quite useful for the assignment of polymer resonances. If the assignments of the carbon spectrum is known, then assignment of the proton spectrum may be made by inspection of the carbon-proton correlation map, as shown by Figure 3. Conversely, assignment of the proton spectrum may lead to the assignments of the carbon resonances. Additionally, the correlation map shows which methylene protons are nonequivalent and which carbon resonances are shifted by the  $\gamma$ -effect. Frequently the carbon spectrum has not been assigned, and it is necessary to make assignments from the proton spectrum alone. We found that it is necessary to use a combination of correlation techniques (COSY,  $^1\text{H}$ - $^1\text{H}$  double-quantum correlation, and RCT) to uniquely define some of the spin systems. Once several of the stereosequences have been assigned, the rest may be assigned by a process of elimination.

This 2D approach to resonance assignments in polymers is simpler than the methods that have been previously used. One approach is to synthesize isotopically labeled

polymers, usually with  $^2\text{H}$  or  $^{13}\text{C}$ . While this method may lead to a direct and unambiguous assignment of the resonance, it can be time consuming and expensive. A simpler, but indirect, approach is to make assignments based on the sequence probabilities and the expected  $\gamma$ -effects on the  $^{13}\text{C}$  chemical shifts. The approach is less successful for proton assignments because the spectrum is less resolved and the peaks are insensitive to the  $\gamma$ -effect.

From these studies it is possible to estimate the degree to which 2D NMR may be used to examine more complex systems, which include defects in the polymer chain and several types of monomer units. Most of the 2D spectra reported here required 9–12 h to acquire. At the lowest contour levels we could just see the correlations to the mmm tetrad sequences, which are present to about 8%. 2D NMR of polymer defects less than 1–2% is probably not feasible unless the properties of the defects are considerably different from those of the main chain. The 2D techniques may be successfully applied to more complex polymer systems as long as the resonances from the various monomers are resolved. The use of experiments such as the relayed coherence transfer makes it possible to correlate through longer sections of the polymer chain. In the study of copolymers we expect that this additional information will remove the ambiguities that may complicate the assignment procedure.

## References and Notes

- (1) Bovey, F. A. "Chain Structure and Conformation of Macromolecules"; Academic Press: New York, 1982.

- (2) Bovey, F. A. "High Resolution NMR of Macromolecules"; Academic Press: New York, 1972.
- (3) Jeener, J.; Meier, B.; Bachmann, P.; Ernst, R. *J. Chem. Phys.* 1979, 71, 4546.
- (4) Bax, A. "Two Dimensional Nuclear Magnetic Resonance in Liquids"; Delft University Press: Delft, Holland, 1982.
- (5) Wider, G.; Macura, S.; Kumar, A.; Ernst, R. R.; Wüthrich, K. *J. Mag. Reson.* 1984, 56, 207.
- (6) Macura, S.; Wüthrich, K.; Ernst, R. *J. Mag. Reson.* 1982, 47, 351.
- (7) Gerig, J. T. *Macromolecules* 1983, 16, 1797.
- (8) Bruch, M. D.; Bovey, F. A. *Macromolecules* 1984, 17, 978.
- (9) Gippert, G. P.; Brown, R. L. *Polym. Bull. (Berlin)* 1984, 11, 585.
- (10) Cheng, H.; Lee, G. *Polym. Bull. (Berlin)* 1984, 12, 463.
- (11) Bruch, M. D.; Bovey, F. A.; Cais, R. E. *Macromolecules* 1984, 17, 2547.
- (12) Macura, S.; Brown, R. L. *J. Mag. Reson.* 1983, 53, 529.
- (13) Brown, R. L. *J. Mag. Reson.* 1984, 57, 513.
- (14) Heatley, F.; Bovey, F. A. *Macromolecules* 1969, 2, 618.
- (15) Carman, C. J.; Tarpley, A. R.; Goldstein, J. H. *J. Am. Chem. Soc.* 1971, 93, 2864.
- (16) Maudsley, A.; Müller, L.; Ernst, R. *J. Mag. Reson.* 1977, 28, 463.
- (17) Bax, A. *Top. Carbon-13 NMR Spectrosc.* 1983, 197.
- (18) Bax, A.; Freeman, R.; Morris, G. *J. Mag. Reson.* 1981, 42, 164.
- (19) Mareci, T. H.; Freeman, R. *J. Mag. Reson.* 1983, 51, 531.
- (20) Kessler, H.; Bernd, M.; Kogler, H.; Zarbock, J.; Sorensen, O. W.; Bodenhausen, G.; Ernst, R. R. *J. Am. Chem. Soc.* 1983, 105, 6944.
- (21) Bolton, P. H. *J. Mag. Reson.* 1982, 48, 336.
- (22) Wagner, G. *J. Mag. Reson.* 1983, 55, 151.
- (23) Flory, P. J. "Statistical Mechanics of Chain Molecules"; Wiley Interscience: New York, 1969.
- (24) Tonelli, A. E.; Schilling, F. C. *Acc. Chem. Res.* 1981, 14, 233.
- (25) Bax, A.; Drobny, G. *J. Mag. Reson.* 1985, 61, 309.

## Effect of Arm Number and Arm Molecular Weight on the Solid-State Morphology of Poly(styrene-isoprene) Star Block Copolymers

David B. Alward,<sup>†</sup> David J. Kinning, and Edwin L. Thomas\*

Department of Polymer Science and Engineering, University of Massachusetts, Amherst, Massachusetts 01003

Lewis J. Fetters

Exxon Research and Engineering Company, Corporate Research Science Laboratories, Clinton Township, Annandale, New Jersey 08801. Received March 25, 1985

**ABSTRACT:** The morphological characteristics of star-branched block copolymers having poly(styrene-isoprene) arms (30 wt % polystyrene) have been examined by using electron microscopy, small-angle X-ray scattering, dynamic mechanical thermal analysis, and vapor sorption studies. The special molecular architecture of the star molecules was found to modify the nature of the microphase-separated solid state. The influence of segment molecular weights and star functionality (where  $f$  ranged from 2 to 18) on the morphology was examined. In certain cases, e.g.,  $f \geq 8$ , branching brings about the formation of an ordered bicontinuous structure; this structure is not seen in linear materials of equivalent compositions where the equilibrium morphology is that of polystyrene cylinders hexagonally packed in the polydiene matrix.

## Introduction

Because of their intrinsic scientific interest and commercial utility, diblock and triblock copolymers have been the subject of intense research since the early 1960s. A clear picture of the morphology of these materials as a function of composition and processing conditions has emerged. However, work on the morphology of star block copolymers is quite limited. This is due to the difficulty

of producing well-defined stars in terms of the dispersity of arm number and arm length (molecular weight). The aim of this paper is to examine star block copolymers with the primary emphasis on determining how the special molecular architecture of star molecules modifies the nature of the microphase-separated solid state. The investigative tools are primarily electron microscopy and small-angle X-ray scattering (SAXS), augmented by dynamic mechanical thermal analysis and vapor sorption studies. The polymer samples consist of a series of carefully synthesized poly(styrene-isoprene) star molecules of constant (30 wt % polystyrene) composition with various

\* To whom correspondence should be addressed.

<sup>†</sup> Present address: Monsanto Polymer Products Co., Springfield, MA 01151.